JOURNAL OF Applied Polymer SCIENCE

Biodegradable Polyester-Based Heat Management Materials of Interest in Refrigeration and Smart Packaging Coatings

Rocio Perez-Masia, Amparo Lopez-Rubio, Maria Jose Fabra, Jose Maria Lagaron
Novel Materials and Nanotechnology Group, IATA-CSIC, Avda. Agustin Escardino 7, 46980 Paterna, Valencia, Spain
Correspondence to: J. M. Lagaron (E-mail: lagaron@iata.csic.es)

ABSTRACT: In this study, two biodegradable matrices, polycaprolactone (PCL) and polylactide (PLA) were used to encapsulate for the first time a phase changing material (PCM), specifically dodecane (a paraffin which has a transition temperature at −10°C), through the use of the electrospinning technique with the aim of developing coating materials with energy storage capacity for thermal insulation applications. The encapsulation efficiency obtained using both matrices has been studied and the different morphology, thermal properties, and molecular structure of the materials developed were characterized. Results showed that dodecane can be properly encapsulated inside both biopolymers with a submicron drop size, albeit PCL provides better encapsulation performance. A temperature mismatch between melting and crystallization phenomena (the so-called supercooling effect) was observed in the encapsulated paraffin, mainly ascribed to the reduced PCM drop size inside the fibers. Addition of dodecanol was seen to best act as a nucleating agent for the PCL/PCM and PLA/PCM structures, allowing a significant amount of heat storage capacity for these systems without supercooling. These innovative ultrathin structured biomaterials are of interest as energy storage systems to advantageously coat or wrap temperature sensitive products in refrigeration equipment and constitute smart food or medical/pharmaceutical packaging.

KEYWORDS: biopolymers and renewable polymers; differential scanning calorimetry; electrospinning; properties and characterization; structure–property relations

Received 5 November 2012; accepted 16 May 2013; Published online
DOI: 10.1002/app.39555

INTRODUCTION

The development of sustainable energy technologies has been intensified over the last years due to the continuous environmental and economic problems related to the energy sources used nowadays. In this field, phase changing materials (PCMs) can be used as energy storage materials, since they are able to absorb or release energy during their melting/crystallization processes. A large number of organic and inorganic materials can be identified as PCMs from their melting temperature. However, they should also present suitable physical, chemical, and kinetic properties. Paraffin compounds fulfill most of these requirements, as they are reliable, predictable, and chemically inert and stable below 500°C. They also show little volume changes on melting and have low vapor pressure in the melt form.[1] Nevertheless, the latent thermal energy storage systems based on PCMs present some drawbacks such as their low thermal conductivity, which limits the energy that can be extracted from them. Another hurdle is their handling, since some PCMs are liquid at ambient temperature and, what is more important; they need to undergo a phase change (i.e., from liquid to solid and vice versa) at the target temperature to exert the desired functionality. Nevertheless, there are some strategies to overcome these difficulties. On the one hand, the PCMs particles' diameter can be reduced to achieve a very high ratio of surface area to volume and, hence, to increase their thermal conductivity.[2] On the other hand, the encapsulation of these particles in a solid matrix allows the easy handling of liquid PCMs.

One innovative approach to encapsulate PCMs, reducing their drop size and controlling the morphology to a submicron scale is by the electrospinning process. This technique uses high voltage electric fields to produce electrically charged jets from viscoelastic polymer solutions. The solutions are dried, by the rapid evaporation of the solvent, producing ultrathin droplets of solid or liquid particles (core material, i.e., the PCM) which are packed into a polymeric matrix (shell material).[3] Thus, ultrathin structures of polymers containing PCMs can be developed to obtain novel thermal storage materials with suitable thermal performances.

Another important parameter which must be controlled during PCMs performance is the so-called supercooling effect, i.e., the lag between the melting and crystallization of the PCM. Generally, supercooling involves a reduction in the crystallization

temperature and, as a result, the latent heat is released at lower temperatures or over a wider temperature range than expected. A more pronounced supercooling has been observed upon micro- and/or nanoencapsulation of the energy storage materials,[4] fact that limits their application. Some strategies have been developed to prevent supercooling, such as addition of nucleating agents to the PCM.

Regarding the matrices for encapsulation, different polymers and biopolymers are currently being tested. Initially, zein, the major storage protein of corn, was researched in our group as a shell material, since it is readily soluble, renewable, and biodegradable and can be electrospun quite easily.[5–8] Additionally, this biopolymer is a food-derived renewable resource that has the ability to form fibers and capsules with enhanced thermal stability properties using electrospinning.[9,10] For this reason, in a previous study,[11] zein was chosen as the matrix to incorporate a PCM into fibers and capsules. Dodecane ($C_{12}H_{26}$) was selected as a PCM because of its advantageous properties as a paraffin and its melting point around −10°C, which could be useful to keep temperature constant in freezing, chilling, storage, and/or transportation systems in different ambits such as food or biomedical, where products are perishable and could be deteriorated if a specific temperature is not kept. Even when only few products may have specific interest at this refrigeration temperature, these studies also serve to demonstrate the potential of the technology for other liquid PCM systems. However, due to the lack of affinity between the polymer and the PCM, one of the main conclusions of this study was that only the coaxial electrospinning configuration was suitable for this system. Additionally, zein is not currently used as a packaging material and has many processability issues. As alternative materials, biopolyesters have lately attracted great industrial interest because of their good physical properties (when compared to other biodegradable and renewable polymers), processability, water resistance, excellent biocompatibility, and commercial availability.[12–15] Biopolyester-based fibrous mats obtained by electrospinning have been developed for a wide number of applications, mainly in the biomedical field for tissue engineering applications or as drug delivery systems.[16–19] However, to the best of our knowledge, the use of biodegradable polyesters to develop energy storage materials has not been reported.

The aim of this study was to overcome all of the previously mentioned issues encountered when using zein as a matrix, by making use of apolar solvents, more easily processable biopolyesters and of the uniaxial electrospinning method. Specifically, polylactic acid (PLA) and polycaprolactone (PCL) were chosen in this study as shell matrices to carry out uniaxial electrospinning encapsulation of dodecane as PCM material.[20] The encapsulation structures developed may be introduced in packaging structures or in refrigeration equipments, in order to obtain smart packaging materials with heat management properties, able to counteract temperature fluctuations and to increase the energetic efficiency of the devices, respectively.

The morphology, the encapsulation efficiency, and the thermal properties of the developed energy storage materials were studied. Moreover, in order to reduce the supercooling of the encapsulated PCM, several nucleating components were introduced in the encapsulated systems. These materials are able to act as first nuclei for dodecane crystallization and thus, facilitate this process. In particular, a nanoclay, a paraffin with a higher melting point than dodecane, and a fatty alcohol were studied. Out of these, the fatty alcohol (dodecanol) was seen the most effective substance to diminish the supercooling effect in these systems, in accordance with the study carried out by other authors.[21,22] Additionally, a temperature-resolved ATR-FTIR methodology has been put forward to compare the behavior of the phase changes at the molecular scale with the bulk calorimetric results during the first order thermal transitions.

EXPERIMENTAL

Materials

A semicrystalline extrusion grade of polylactic acid (PLA; Natureworks) with a D-isomer content of approximately 2% was used in this study. This biopolymer had a weight average molecular weight (*Mw*) of 150,000 g/mol and a number average molecular weight (*Mn*) of *ca.* 130,000 g/mol. The polycaprolactone (PCL) grade FB100 was kindly supplied in pellet form by Solvay Chemicals (Belgium). This grade had a density of 1.1 g/cm^3 and a mean molecular weight of 100,000 g/mol. Dodecane and *N,N*-dimethylformamide (DMF) with 99% purity were purchased from Sigma-Aldrich (Spain). Trichloromethane was purchased from Panreac Quimica S.A. (Spain). Regarding the nucleating agents, a food contact compliant organo-modified bentonite clay commercially marketed as O_2Block from Nanobiomatters S.L. (Paterna, Spain), tetracosane ($C_{24}H_{50}$) from Sigma-Aldrich (Spain) and dodecanol from Sigma-Aldrich (Spain) were used.

Preparation of Biopolyesters-PCM Solutions

The electrospinning solutions were prepared by dissolving the required amount of PLA and PCL, under magnetic stirring, in a solvent prepared with a mixture of trichloromethane : *N,N*-dimethylformamide (85 : 15 w/w) in order to reach a 5 or 15% in weight (wt %) of PLA or PCL, respectively. Afterwards, 20 wt % or 45 wt % of PCM (dodecane) with respect to the polymer weight was added to the PLA or PCL solutions, respectively, and stirred at room temperature until it was completely dissolved. For the biopolymer/PCM solutions prepared with a nucleating agent, this was first dissolved in the PCM under magnetic stirring before being added to the PLA or PCL solution.

Characterization of Biopolyesters-PCM Solutions

The viscosity and surface tension of all the biopolymeric solutions were characterized before the electrospinning process. The viscosity was determined by a rotational viscosity meter VISCO BASIC PLUS L with a Low Viscosity Adapter (spindle LCP) from Fungilab S.A. (Spain). The surface tension was measured with a tensiometer "EasyDyne" from Krüss (Germany) using the Wilhelmy Plate method. Both measurements were done, in triplicate, at 25°C.

Preparation of the Biopolyesters-PCM Fibers Through Electrospinning

The electrospinning apparatus, equipped with a variable high-voltage 0–30 kV power supply, was a Fluidnatek® basic setup assembled and supplied by BioInicia S.L. (Valencia, Spain). PCL/PCM or PLA/PCM solutions were introduced in a 5 mL glass syringe and were electrospun under a steady flow-rate using a stainless-steel needle. The needle was connected through a PTFE wire to the syringe. The syringe was lying on a digitally controlled syringe pump while the needle was in horizontal towards a copper grid used as collector. The electrospinning conditions for obtaining both PCM-containing biopolymer structures were optimized and fixed at 1 mL/h of flow-rate, 12.5 kV of voltage and a tip-to-collector distance of 10 cm.

Scanning Electron Microscopy (SEM)

The morphology of the electrospun fibers was examined using SEM on a Hitachi microscope (Hitachi S-4800) after having been sputtered with a gold-palladium mixture in vacuum. All SEM experiments were carried out at 5 kV. Fiber diameters were measured by means of the Adobe Photoshop CS4 software from the SEM micrographs in their original magnification.

Differential Scanning Calorimetry (DSC)

Thermal analysis of electrospun fibers were carried out on a DSC analyzer (Perkin Elmer DSC 7, US) from −40 to 10°C in a nitrogen atmosphere using a refrigerating cooling accessory (Intracooler 2, Perkin Elmer, US). The scanning rate was 2°C/min in order to minimize the influence of this parameter in the thermal properties. The amount of material used for the DSC experiments was adjusted so as to have a theoretical dodecane content of 1–2 mg approximately. The enthalpy results obtained were, thus, corrected according to this PCM content. Measurements were done in triplicate.

Attenuated Total Reflectance Infrared Spectroscopy (ATR-FTIR)

ATR-FTIR spectra of biopolyester fibers, pure dodecane, and electrospun biopolyesters–dodecane structures were collected at different temperatures coupling the low temperature Golden Gate Diamond ATR system accessory (Specac, UK) to FTIR Tensor 37 (Bruker, Germany) equipment. Temperature was controlled by the 4000 Series High Stability Temperature Controller accessory (Specac, UK). The spectra were collected in the pressed materials from −35 to 10°C by averaging 7 scans at 4 cm^{-1} resolution. The spectra obtained at room temperature (20°C) were collected by averaging 20 scans at 4 cm^{-1} resolution. The experiments were repeated twice to verify that the spectra were consistent between individual samples.

Nuclear Magnetic Resonance (NMR)

NMR analyses were done, in triplicate, in order to estimate the PCM loading in the biopolymeric fibers. Initially, a calibration curve was obtained by recording the NMR data of the pure polymeric fibers, pure dodecane, and different mixtures of polymeric fibers/dodecane. Specifically, the polymer fibers : PCM mass range of the mixtures were 90 : 10, 70 : 30, and 50 : 50. The materials were dissolved in deuterated chloroform ($CDCl_3$) and subjected to the NMR analyses. The spectra were collected at 300.13 MHz (^1H) in a DPX 300 equipment (Bruker, Germany) with controlled temperature (25°C) and 128 scans. The ratio of the polymers to the paraffin was calculated from the ratio of the integration of resonance peaks which represent the polymer chains (δ of 2.40–2.25 ppm of the adjacent protons to the carbonyl group for PCL and δ of 5.30–5.00 ppm of the –CH groups for PLA) and those for dodecane (δ of 1.40–1.15 ppm of the $–CH_2$ groups of dodecane). The calibration curves obtained were:

$$y = -11.5 \ln(x) + 24.9 \text{ (for PCL structures)} \quad (1)$$

$$y = -12.6 \ln(x) + 14.9 \text{ (for PLA materials)} \quad (2)$$

Where "y" was the concentration of PCM included in the fibers and "x" was the calculated ratio of the integration of resonance peaks. Then, the hybrid electrospun biopolyesters-dodecane structures were analyzed using the same conditions and the dodecane loading of the fibers was estimated from the calibration curves.

Thermogravimetric Analysis (TGA)

Compositional analysis of the fibers was also carried out according to the method proposed by Desai et al.[23] using a TA Instruments model Q500 TGA. The pure polymers (PLA and PCL) and the hybrid electrospun mats were weighed (*ca.* 20 mg) and heated from 20 to 600°C with a heating rate of 10°C/min under nitrogen atmosphere. The weight loss for the polymers and the paraffin in the hybrid fibers was evaluated by taking the first-order derivative of the weight loss thermograms. The area under the respective degradation temperature peaks is related to the polymer/pcm content in the blends.

Statistical Analysis

Statistical analysis of the data was performed through analysis of variance (ANOVA) using Statgraphics Plus for Windows 5.1 (Manugistics, Rockville, MD). Fisher's least significant difference (LSD) procedure was used at the 95% confidence level.

RESULTS AND DISCUSSION

Solution Properties and Morphology of the Electrospun Structures

Based on screening studies on the electrospinning of the biopolyesters, the concentrations of PCL and PLA were optimized to obtain stable hybrid fibers containing dodecane (PCM). The optimum concentrations of the biopolymers in the solutions were found out to be 15 wt % for PCL and 5 wt % for PLA. Regarding the PCM concentration incorporated in the solutions, a screening study was also carried out in order to optimize this parameter, and it was observed that PLA structures were not able to encapsulate large amounts of dodecane and thus, only 20 wt % of PCM respect to the polymer could be incorporated. On the other hand, PCL structures facilitated the encapsulation of 45 wt % of dodecane within the fibers. Higher fractions tended to destabilize the encapsulation process for the selected polymer/PCM systems. Both the viscosity and surface tension of PCL/PCM and PLA/PCM solutions play an important role in determining the range of concentrations from which continuous fibers can be obtained. Generally, at low viscosities, surface tension is the dominant factor and just beads or beaded fibers are formed, while above a critical concentration, continuous fibrous structures can be obtained, being their morphology affected by

Table I. Viscosity and Surface Tension Values of the Hybrid Biopolymeric Solutions and Pure Dodecane

Sample	Surface Tension (mN m^{-1})	Viscosity (cP)
PCL/PCM	27.6 ± 0.4[a]	876.4 ± 20.9[a]
PLA/PCM	28.4 ± 0.5[a]	42.8 ± 1.3[b]
PCM	24.7 ± 0.0[b]	1.0 ± 0.0[c]

a–cDifferent superscripts within a column indicate significant differences among dodecane and hybrid structures ($P < 0.05$)

the polymer concentration in the solution.[3,22] Table I shows the viscosity and surface tension values of PLA/PCM and PCL/PCM solutions and for pure PCM. The viscosity of the PCL solution was over 20 times higher than the PLA one, as this physical parameter is directly related with the total solids concentration in the final solution, which was greater for the PCL solution. However, the type and the concentration of biopolymer did not significantly affect the surface tension values. The viscosity and surface tension values of the PCM were significantly lower than those obtained for PLA and PCL solutions.

The morphology of the fibers was analyzed through scanning electron microscopy (SEM). Figure 1 shows SEM images of the various hybrid fibers obtained. The fibers obtained from the PCL solution were thicker (up to 1 μm) while PLA solutions generated thin beaded fibers with an average diameter under 200 nm. These differences in fiber diameter can be explained by the greater viscosity of PCL solutions.[3]

Figure 2 shows the cross-sections of pure PCL and PCL/dodecane cryofractured fibers. From these images, it can be observed that the pure PCL fiber was solid and without shafts. However, the incorporation of dodecane led to the formation of multiple channels (indicated with arrows) inside the fibrillar structures where the PCM was supposed to be allocated. For the PLA/dodecane fibers, it was not feasible to obtain detailed SEM images of the cross-sections due to the smaller fiber diameter. Nevertheless, it could be assumed that the distribution of the PCM along the structures occurred in a similar way as in the PCL-based electrospun structures.

Thermal Properties and Molecular Changes of Electrospun Structures

The thermal behavior of the electrospun structures as well as their associated molecular changes during dodecane phase transitions was analyzed by DSC and temperature-resolved ATR-FTIR spectroscopy, respectively. DSC analysis was also used to ascertain the degree of PCM incorporation.

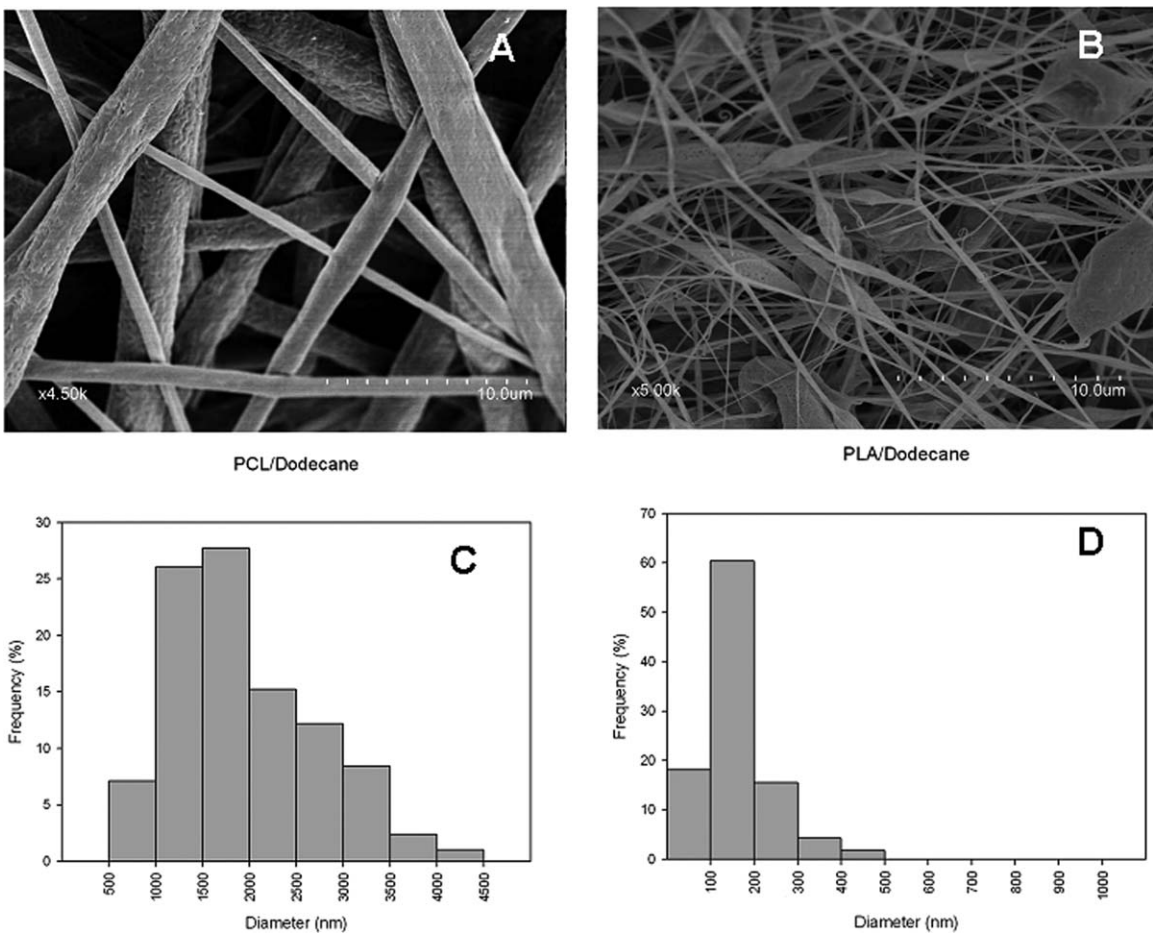

Figure 1. Selected SEM images (A and B) and size distribution (C and D) of PCL/PCM (left) and PLA/PCM (right) fibers. The scale markers correspond to 10 μm.

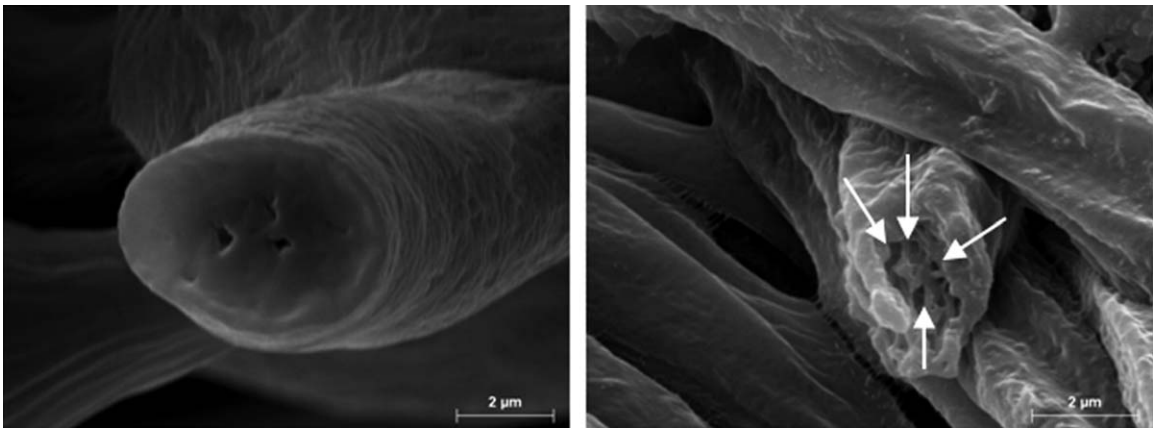

Figure 2. Cross-section SEM images of pure PCL (left) and PCL/PCM (right) fibers. The scale markers correspond to 2 μm. Arrows indicate the channels where PCM is supposed to be located.

Thermal properties (enthalpy values, melting and crystallization temperatures, and supercooling degree) of the pure dodecane and of the hybrid electrospun materials analyzed by DSC at 2°C/min are given in Table II.

From the DSC results, it was observed that pure dodecane melted at −9°C and crystallized at −11.9°C in a narrow temperature range, having an enthalpy of 196.9 J/g. This result is in accordance with other authors.[23]

Figure 3 shows the ATR-FTIR spectra of the pure polymeric fibers, the pure dodecane, and the hybrid electrospun materials analyzed at 20°C. At this temperature, the pure dodecane is characterized by the $–CH_2$ and $–CH_3$ stretching vibration bands at 2957, 2922, and 2852 cm^{-1}. These bands were also observed in the PLA and PCL hybrid structures even though they were overlapped with spectral bands from the biopolymeric structures, thus confirming the PCM encapsulation in both polymeric matrices.

Furthermore, melting and crystallization behavior of dodecane deposited as a liquid over the ATR crystal was also followed using ATR-FTIR spectroscopy since there are specific spectral changes which correlate with conformational changes of paraffins during their phase transition.[25] Specifically, as observed in this study, the melting process of non-encapsulated dodecane was mainly characterized by the disappearance of the factor group splitting at 2960 and 2952 cm^{-1}, the displacement of the band from the symmetrical stretching vibration of its $–CH_3$ group at 2913 cm^{-1} towards higher wavenumbers and by the continuous drop of the band observed at 716 cm^{-1} until it disappeared. The factor group splitting is the splitting of bands in the vibrational spectra of crystals due to the presence of more than one (interacting) equivalent molecular entity in the unit cell of certain symmetries and has been previously observed in other *n*-alkanes in other frequency regions.[26,27] The existence of a unique band at 716 cm^{-1} in the solid state of dodecane indicates that when the crystal is formed, it presents the triclinic structure typical of even numbered *n*-paraffins with $n \leq 26$.[25] Therefore, these conformational changes were analyzed through ATR-FTIR experiments as a function of temperature in the pure PCM and in the hybrid electrospun structures and the results were compared with the DSC data.

For pure dodecane, as observed in Figure 4(A), the spectral changes associated to the melting of the paraffin took place around −9°C in agreement with DSC results. In contrast, during the cooling scan, ATR-FTIR spectra [Figure 4(B)] showed that the splitting of the band at 2957 cm^{-1} into two components, at 2952 and 2959 cm^{-1} (factor group splitting), as well as the appearance of the band at 716 cm^{-1} occurred at −7°C. These changes suggest that there are conformational changes associated to molecular order taking place at this temperature during the ATR-FTIR run. In contrast, the onset temperature of crystallization as measured by DSC was −11.8°C. These results are in agreement with previous literature showing that the crystallization temperature detected by IR spectroscopy was higher than that obtained through DSC.[25] The differences observed in the onset of crystallization determined by both characterization techniques could, perhaps, be explained by the fact that, in the case of the DSC, the experiment was carried out in nitrogen atmosphere in a closed chamber while the ATR accessory was exposed to the ambient humidity. During cooling in the vicinity of 0°C, ice crystals could form on the ATR surface, which may act as heterogeneous nucleating sites that could promote early dodecane crystallization. The -OH stretching band at *ca.* 3580 cm^{-1} associated to water could be seen in the spectra of dodecane, thus adding strength to this hypothesis (results not shown). Additionally, it is also possible that the ATR crystal surface could promote additional nucleation sites for the PCM layer immediately in contact with the crystal.

The thermal properties of dodecane varied when this PCM was encapsulated in both biopolyester matrices. From Table II, it can be seen that when dodecane was encapsulated in PLA, there was more variability among the enthalpy values of the different samples and the melting temperature was lower than that of non-encapsulated dodecane. This fact could be explained by the reduced PLA fibers average diameter (Figure 1), leading to the formation of smaller or more defective dodecane crystals and, probably, to a heterogeneous distribution of the PCM along the fibers. In contrast, more homogeneous enthalpy values and no variation in the melting temperature (if compared with non-encapsulated dodecane) were obtained for the PCL/dodecane

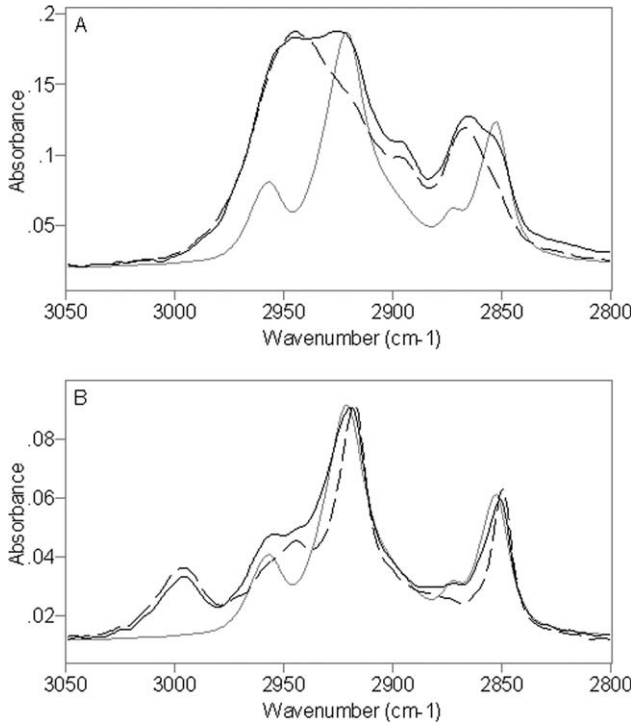

Figure 3. ATR-FTIR spectra of the pure polymers (black dashed line), pure dodecane (grey line) and hybrid electrospun materials (black solid line) for (A) PCL and (B) PLA structures.

systems, which allowed an easier PCM encapsulation. Nevertheless, in both biopolyester-based encapsulation structures, the melting process occurred over a broader temperature range than in pure dodecane (peak width of ~3°C for the encapsulated dodecane vs. ~1°C for the bulk paraffin), probably because in the encapsulated systems there was a greater heterogeneity of crystallites due to the different crystallization mechanisms, as it will be explained later, and also because the polymers themselves could be hindering heat transfer across the structures, thus prolonging the melting event.[29] In contrast with the similarities in the melting temperature between bulk and encapsulated dodecane, the crystallization event was considerably different. While pure dodecane crystallized at −11.98°C, a greater supercooling degree was observed in both PCL and PLA capsules. The supercooling effect was probably due to the reduction of the PCM particle size, since the number of nuclei needed to initiate the crystallization process decreased with reducing the diameter of the dodecane drops inside the fibers.[4] Moreover, a multiple crystallization profile was seen for encapsulated dodecane and, specifically, two and three crystallization temperatures were detected for the hybrid PCL and PLA structures, respectively. Multiple crystallization processes have been attributed to the rotator phase transition, which is observed in some *n*-alkanes when their particle size is reduced.[30] A rotator phase is defined as lamellar crystals, which exhibit long-range order in the molecular axis orientation and center-of-mass position but lack rotational degrees of freedom of the molecules about their long axis.[31] In these cases, more than one peak is observed in the DSC analysis

Table II. Thermal Properties of Pure Biopolyesters, PCM, and Biopolyester/PCM Structures

Samples	ΔH_m (J/g)	T_m (°C)	ΔH_c (J/g)	T_{c1} (°C)	T_{c2} (°C)	T_{c3} (°C)	Supercooling (°C)
PCL	55.77 ± 5.0	55.55 ± 1.9	−51.05 ± 1.2	30.95 ± 1.9	-	-	-
PLA	28.52 ± 6.9	147.93 ± 5.1	−17.39 ± 2.3[a]	91.87 ± 0.6[a]	-	-	-
PCM	196.88	−9	−199.03	−12	-	-	2.98
PCL/PCM	73.71 ± 2.2[a]	−8.31 ± 0.6[a]	−73.87± 2.8 [a]	−13.53 ± 0.4 [a]	−23.03 ± 0.4 [a]	-	5.22 ± 1.09 [a]
PLA/PCM	20.08 ± 4.1[b]	−9.71 ± 0.1[b]	−23.15 ±4.3 [b]	−23.36 ± 0.3 [b]	−29.12 ± 2.3 [b]	−38.98 ± 0.9 [a]	13.65 ± 0.28 [b]

ΔH_m: Melting enthalpy; T_m: Melting temperature; ΔH_c: Crystallization enthalpy; T_{c1}, T_{c2}, T_{c3}: Crystallization temperatures.
[a,b]Different superscripts within a column indicate significant differences between biopolyester/PCM structures ($P < 0.05$).
[a]These values refer to the cold crystallization transition of PLA.

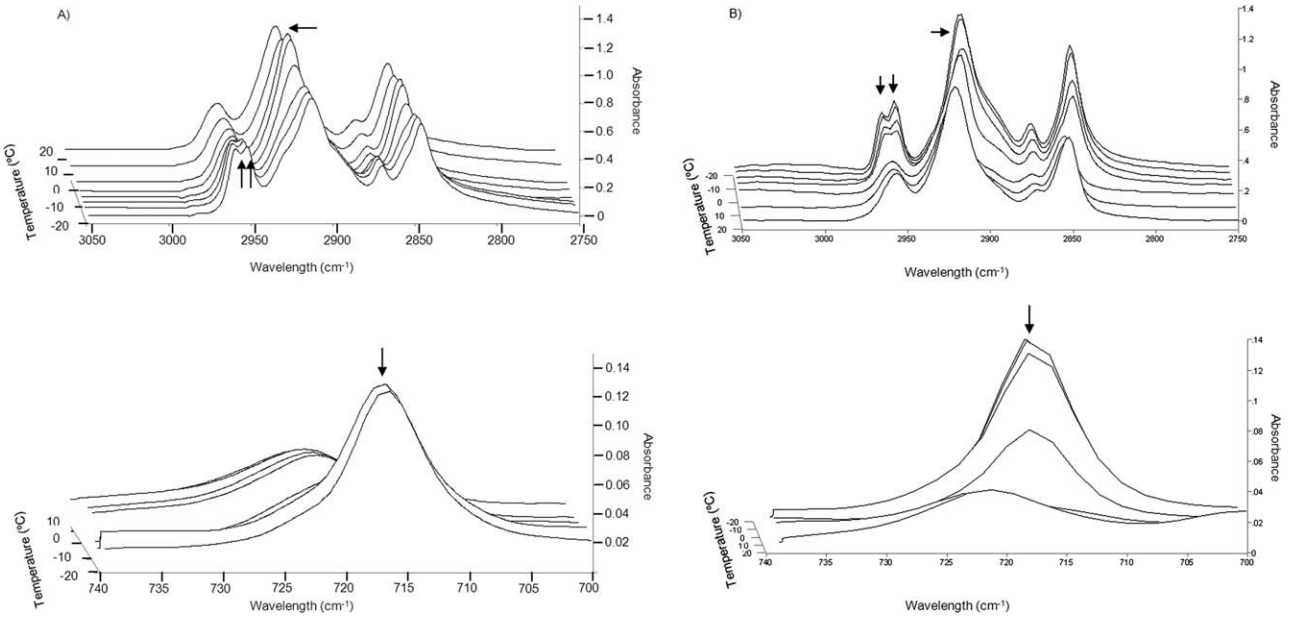

Figure 4. ATR-FTIR spectra of pure dodecane at different temperatures during (A) heating and (B) cooling. Arrows indicate the evolution of factor group splitting, the displacement of the band at 2916 cm^{-1} and the evolution of the band at 716 cm^{-1}.

during the crystallization process due to the different kind of crystals attained depending on the crystallization mechanism followed. The first peak belongs to the heterogeneously nucleated liquid-rotator transition, the second one includes the rotator-crystal transition and the last one is attributed to the homogeneously nucleated liquid-crystal transition. Sometimes the second and third transitions appear as a single peak,[30] as was the case here for the hybrid PCL/dodecane structures.

In a similar way as with pure dodecane, the hybrid PCL and PLA structures were also analyzed by ATR-FTIR spectroscopy in order to better understand the conformational changes occurring during the phase transitions. It is of particular interest to realize that, in order to get a proper ATR signal, the samples had to be pressed against the ATR crystal, which was not a requirement for the case of the liquid neat PCM experiment described above. As with pure dodecane, the spectral changes associated with the melting event for both encapsulation structures occurred at the same temperatures observed through DSC, although they were observed over a broader temperature range (results not shown). This could be explained on the bases of infrared spectroscopy being able to pick up conformational changes beyond first order melting/crystallization transitions and may also be more sensitive to ill-defined lateral order phenomena compared to DSC.[23]

Regarding the crystallization of dodecane within the electrospun biopolyesters, it was mainly followed through the increase in the FTIR band at 2950 cm^{-1} related to the factor group splitting [cf. arrows in Figures 5(A,B)] and through the displacement of the band at 2922 cm^{-1}. Figure 5 displays the temperature-resolved crystallization spectra (from 3050 to 2970 cm^{-1}) and the wavenumber versus temperature plot for the band at 2922 cm^{-1} of PCL/PCM and PLA/PCM fibers.

In the case of the PCL/PCM fibers, it was seen that a band at 2950 cm^{-1} appeared at −13°C and its intensity continuously increased during the cooling scan [Figure 5(A)]. The same event was observed in the PLA/PCM structures [Figure 5(B)], which became obvious at −10°C, when an increase in the band at 2951 cm^{-1} was observed. The band was not clearly seen until −15°C in agreement with the rise in band intensity observed for the pure component. These results seem to indicate that some conformational changes of dodecane were taking place from −10°C. However, crystallization as such, required lower temperatures, probably as a result of the discussed reduction in drop size due to encapsulation. Regarding the displacement of the band at 2922 cm^{-1}, from Figure 5(A), it can be seen that for PCL hybrid structures there were three sharp changes during the shift of this band, taking place at −14, −20, and −25°C, approximately. These three jumps could be related with the corresponding rotator states defined earlier, although DSC was not able to detect separately the second and third one. For PLA/PCM fibers, Figure 5(B) shows that the abrupt changes along the displacement of the band at 2922 cm^{-1} were detected at −12, −25, and −30°C and these changes could also be related with the different rotator states. The fact that the crystallization temperatures detected with the spectroscopic technique were slightly higher than those obtained through DSC could be attributed, as previously mentioned, to a potentially greater nucleation effect promoted by ice crystals and/or by the ATR crystal itself. Moreover, these samples were pressed over the ATR crystal which could also affect the phase transition temperature, as it can be observed from a typical phase diagram.[32,33]. From phase diagrams, it can be observed that for a fixed temperature, the material state changes if pressure is modified, i.e., when increasing the pressure, the paraffins can be in solid state, even though the temperature is higher than their crystallization temperature. Although phase diagrams only

Applied Polymer SCIENCE

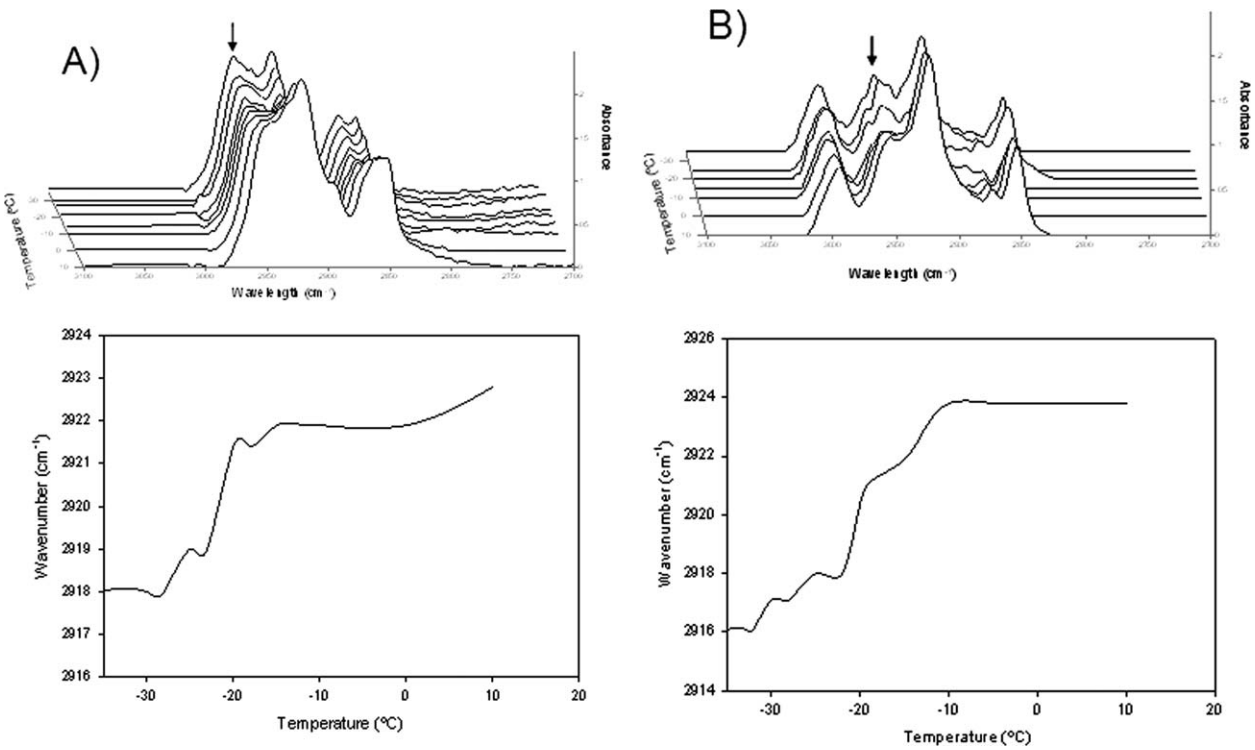

Figure 5. ATR-FTIR crystallization spectra of (A) PCL/PCM and (B) PLA/PCM structures at different temperatures and the wavenumber versus temperature plot for the band at 2922 cm^{-1} of PCL/PCM (A) and PLA/PCM (B) fibers.

describe ideal systems, the effect of pressure on the crystallization temperature of some alkanes in real systems has been already reported by some authors.[32,33]

Evaluation of the PCM Encapsulation Efficiency and Loading

The PCM encapsulation efficiency and loading capacity of the polymeric fibers was evaluated from the enthalpy results obtained through DSC and also by NMR and TGA. The encapsulation efficiency through DSC was calculated by dividing the theoretical melting enthalpy of the hybrid materials by the experimental melting enthalpy obtained for these materials. The theoretical melting enthalpy was obtained considering the quantity of the PCM added to the electrospinning solution (45 or 20%) and multiplying this factor by the enthalpy of the pure dodecane. Table III shows the encapsulation yield derived from the DSC results of both biopolymeric matrices and the calculated total amount of dodecane encapsulated in these two fiber systems. According to DSC, PCL structures presented greater encapsulation efficiency than PLA fibers. Therefore, for PCL/dodecane structures, an encapsulation efficiency of 83% was achieved, which means that the capsules are composed by ~37 wt % of PCM (the core material) and ~63 wt % of the PCL shell material. Thus, the energy storage of the encapsulation system (considering both the PCM and the PCL) was around 72 J/g of material which is similar to some PCM products currently commercialized for dealing with room and human comfort range temperatures.[40,41] On the other hand, according to DSC, only a 10 wt % of the PCM was providing energy storage capacity in the PLA structures, thus having a considerably lower energy storage capacity (~20 J/g).

In order to confirm the encapsulation efficiency results obtained through DSC, the hybrid electrospun materials were subjected to NMR analyses using integration of resonance peaks from the polymer chains (at δ of 2.40–2.25 ppm of the adjacent protons to the carbonyl group for PCL and δ of 5.30–5.00 ppm of the —CH groups for PLA)[34,35] and those from dodecane (δ of

Table III. PCM Encapsulation Content and Efficiency as Inferred by DSC and of the Content as Determined by NMR and TGA

	DSC		NMR		TGA
Samples	PCM (wt %)	Efficiency (%)	Peaks ratio[a]	PCM (wt %)	PCM (wt %)
PCL/PCM	37.44 ± 1.1	83	0.29 ± 0.2	39.12 ± 3.7	35.86 ± 0.93
PLA/PCM	10.20 ± 2.1	51	0.67 ± 0.1	19.76 ± 2.3	19.60 ± 0.99

[a] Ratio of the integration of resonance peaks from the biopolyesters (δ of 2.40–2.25 ppm of the adjacent protons to the carbonyl group for PCL and δ 5.30–5.00 ppm of the –CH groups for PLA) and dodecane (δ of 1.40–1.15 ppm of the $-CH_2$ groups).

Table IV. TGA Maximum of the Weight Loss First Derivate for the PCM Dodecane (T_{D1}) and the Biopolyesters (T_{D2}) and the Corresponding Peak Onset and Endset Values for Dodecane (T_1) and the Biopolyesters (T_2)

Samples	Onset T_1 (°C)	T_{D1} (°C)	Endset T_1 (°C)	Onset T_2 (°C)	T_{D2} (°C)	Endset T_2(°C)
Dodecane	40.5	197.1	210.5	-	-	-
PLA	-	-	-	265.9	340.8	370.7
PCL	-	-	-	322.9	410.8	472.1
PLA/PCM	75.7	152.9	226.1	247.9	334.5	367.4
PCL/PCM	77.9	189.2-209.4	272.9	319.4	409.2	471.6

1.40–1.15 ppm of the —CH_2— groups of dodecane).[36] Although, the NMR technique does not provide accurate quantitative information, it can be useful to estimate a range of values for the PCM loading levels.[37] The NMR assays were done in the liquid state favoring the release of the dodecane because of the complete dissolution of fibers and, thus, these results were expected to provide a more accurate data regarding dodecane loading than the indirect DSC data. The results are compiled in Table III and show that while the PCM loading level for the PCL/PCM fibers was closer to the results obtained through DSC (~39 wt % of dodecane encapsulated), in the case of the PLA/PCM electrospun materials the dodecane loading results were very different depending on the technique used. While NMR provided a PCM loading of around 20%, according to the enthalpy results from DSC the loading inferred was just around 10%. This might be explained by the fact that the intrinsic morphology of the obtained PLA fibers, which were considerably thinner, could impede the complete crystallization of the encapsulated dodecane. In view of the results, it is hypothesized that a fraction of encapsulated dodecane does never crystallize, most likely because the undercooling required is larger than the one applied or because it interacts with the polymer in very small confined moieties. This also happened but to a much smaller degree for PCL since 45% of the PCM was theoretically encapsulated while only *ca.* 37% provided energy storage capacity.

To further estimate the loading content of the hybrid PCM/biopolyester fibers, TGA was used. The derivative curves from the pure polymers (PLA and PCL) and from the paraffin showed separate decomposition temperatures and, when the hybrid fibers were analyzed it was also possible to distinguish between the decomposition curves of the biopolyester and the PCM. Table IV compiles the maximum of the weight loss first derivative (T_D) and the corresponding peak onset and endset values for the pure compounds and hybrid fibers obtained from the TGA curves.

From Table IV, it can be observed that both the onset and endset temperatures of dodecane degradation were displaced towards higher temperatures when the PCM was within the electrospun fibers. However, the effect of the paraffin in the thermal stability of the biopolyesters was different and, while a slight decrease in the thermal stability of PLA was observed in the hybrid fibers, no significant changes in the thermal degradation parameters were seen for PCL fibers. In any case, it was possible to clearly distinguish two different degradation curves (the first one corresponding to the PCM and the second one to the biopolyester) in the hybrid fibers. Through the integration of the areas of the corresponding peaks it was possible to estimate the PCM loading in the electrospun fibers (Table III). When this method was used, the PCM content of the PLA and PCL fibers was calculated to be ~19.6 and ~35.9%, in agreement with the NMR data. These results confirm that, in the case of PLA, the encapsulation efficiency was greater than that calculated through DSC.

Diminishing the Supercooling Effect

In order to reduce the supercooling effect in the encapsulated structures, different nucleating agents were added to dodecane. Thus, a nanoclay, tetracosane, and dodecanol were tested. All of these substances were solid at the crystallization temperature of dodecane and, thus, they were thought to act as first nuclei for the crystallization process. Figure 6 shows the reduction in supercooling of the nucleating agents assayed. From this figure, it is observed that dodecanol was seen to act as the most suitable nucleating agent, and thus it was selected for doing a more exhaustive study.

Figure 7 shows the thermograms of (a) the pure PCM (b) the PCM with 10% of dodecanol and (c) the PCL/PCM fibers (d) and the PLA/PCM fibers with 5 and 10% of dodecanol, respectively. From Figure 7(a) and (b), it is seen that the melting

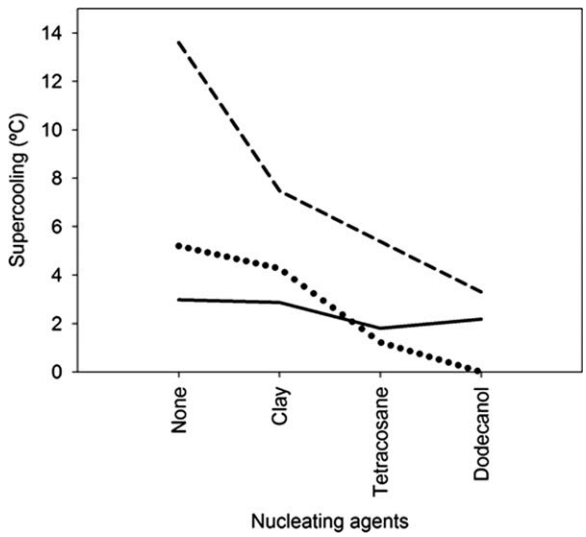

Figure 6. Effect of the nucleating agents in the supercooling for dodecane (solid line), PCL/dodecane (dotted line), and PLA/dodecane (dashed line).

Applied Polymer SCIENCE

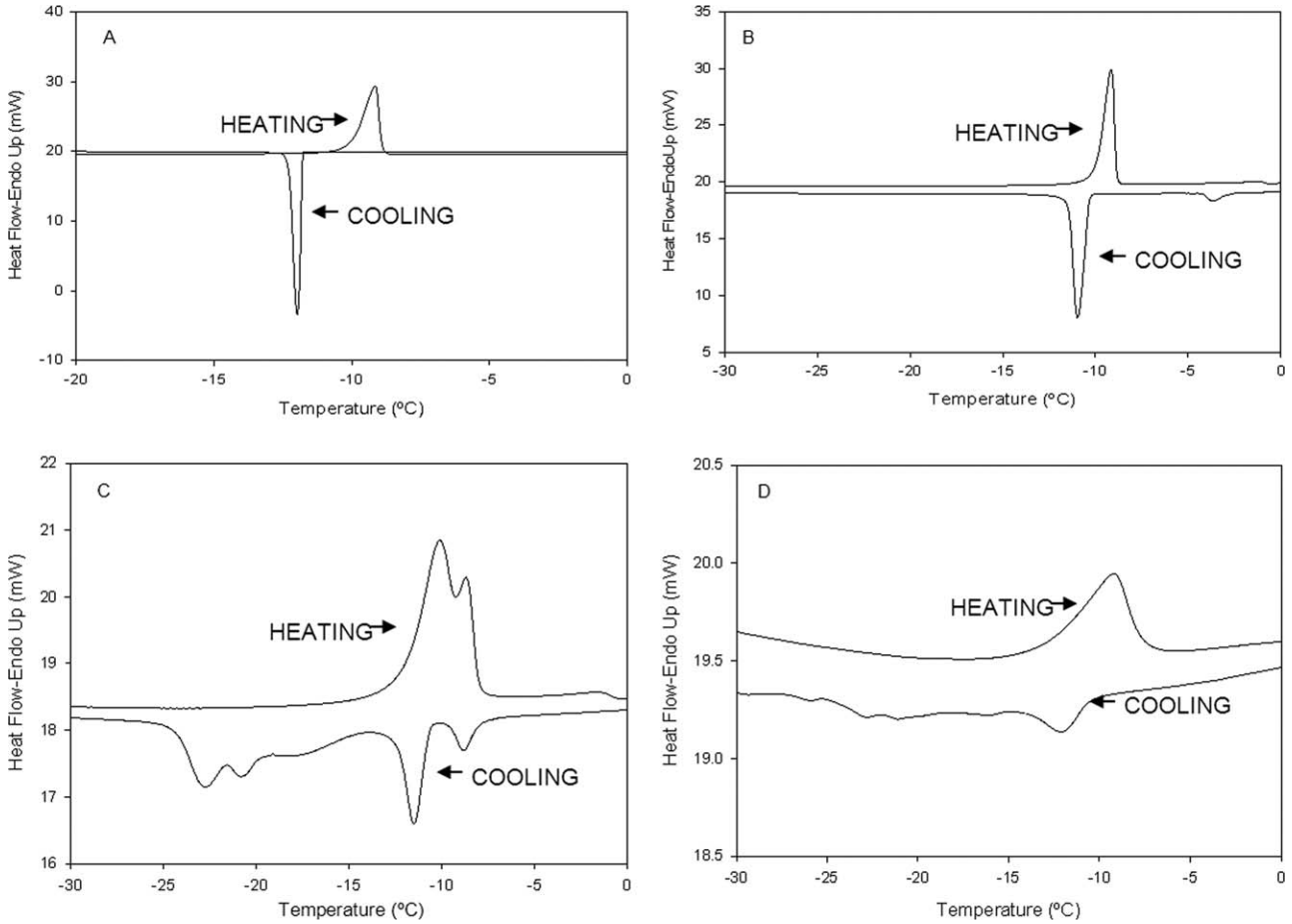

Figure 7. DSC thermograms of (a) pure PCM, (b) PCM with 10 wt % dodecanol, (c) PCL/PCM fibers with 5 wt % dodecanol, and (d) PLA/PCM fibers with 10 wt dodecanol.

process of the PCM with 10% of dodecanol occurred in a wider temperature range (from −9.6 to −0.7°C approximately) than for the pure PCM. This melting behavior is associated with the precipitation of redundant dodecanol in dodecane near the melting point of dodecane, as it was reported before by Fan and coworkers with octadecane and octadecanol.[38,39] When the PCM with dodecanol was encapsulated inside the PCL structures [Figure 7(c)], two overlapping melting peaks were observed probably due to heterogeneous crystal formation as a consequence of dodecanol addition. However, this was not observed in PLA/PCM fibers additivated with 10% of dodecanol [Figure 7(d)] where only one melting peak was observed. Similarly to the result shown in the PCM/dodecanol mixture [Figure 7 (b)], the thermograms of PCL/PCM and PLA/PCM structures prepared with the nucleating agent also presented a melting shoulder expanding over a broad temperature range.

Table V shows crystallization temperatures obtained by DSC and the percentage of latent heat released at each temperature in both, PCL/PCM and PLA/PCM electrospun fibers prepared with different amounts of dodecanol (0, 5 and 10 wt %). The enthalpy results showed that addition of 5 and 10 wt % of dodecanol to PCL/PCM structures favored the release of 40% and 55% of the latent heat without supercooling, respectively. However, when the amount of nucleating agent was increased to 10 wt %, part of the heat was released close to 0°C, which is far from the target temperature expected for the application of these materials. For PLA/PCM structures, the effect of dodecanol was slightly different. Specifically, for this matrix, it was observed that addition of a 5 wt % of nucleating agent was not effective in reducing supercooling; however, when 10 wt % dodecanol was included within the fibers, a 35% of the PCM crystallized without supercooling. Therefore, these results further confirm that crystallization of dodecane was favored in thicker structures (such as the ones obtained with PCL), whereas in the thinner PLA structures it was necessary to add a greater amount of nucleating agent to facilitate the crystallization of the PCM.

CONCLUSIONS

In this study, heat management materials were successfully developed based on the encapsulation of a PCM (dodecane) inside biodegradable polyesters (PCL and PLA) by means of the electrospinning technique. PCL/dodecane fibers were considerably thicker than the PLA/dodecane encapsulates obtained. The hybrid materials made from PCL were able to encapsulate a greater amount of dodecane than those obtained with PLA. Regarding the thermal properties, it was observed that the melting behavior of the encapsulated PCM was similar as for the

pure PCM. However, the crystallization was affected by the encapsulation process because of the reduced size of the PCM pockets obtained and, generally, higher supercooling was observed in the developed electrospun structures. Nevertheless, the addition of a nucleating agent was able to minimize this effect. Regarding to the efficiency of the process, the PCM efficiency and loading in the fibers was measured by DSC, TGA, and NMR. Results showed that PCL fibers were able to encapsulate a heat storage capacity equivalent to ~37 wt % of the PCM. However, for the PLA materials, the dodecane loading results were different depending on the technique used. While NMR and TGA provided an encapsulation loading of around 20 wt %, according to the results from DSC, the heat storage capacity was equivalent to a loading of 10 wt % of the PCM. The differences in the latter case were ascribed to a fraction unable to crystallize inside the PLA matrix. Nevertheless, the structures developed presented improved properties with respect to the neat PCM, since in the encapsulated systems there was a fraction of the PCM which showed no supercooling effect. Thus, these systems could be of significant interest in energy storage and thermal insulation applications. In particular, the materials produced within this study could be applied as coatings for refrigeration machinery or for food/biomedical packaging where low temperatures are required to keep an optimum product quality.

Table V. Thermal Properties of the Electrospun PCL/PCM and PLA/PCM Fibers Prepared with Dodecanol

Samples	% Dodecanol	T_m (°C)	T_{c1} (°C)	ΔH_1 (%)	T_{c2} (°C)	ΔH_2 (%)	T_{c3} (°C)	ΔH_3 (%)	Supercooling (°C)
PCL/PCM	0	-8.3 ± 0.6^{a}	-13.5 ± 0.4^{a}	65.2 ± 8.0	-23.0 ± 0.4^{a}	34.8 ± 8.1	-	-	5.2 ± 1.1
	5	-9.4 ± 0.3^{abc}	-7.9 ± 0.8^{b}	10.0 ± 3.3	-12.6 ± 2.2^{b}	29.1 ± 5.0	-22.4 ± 0.4^{a}	60.9 ± 8.3	1.5 ± 0.7
	10	-8.7 ± 0.5^{ab}	-2.1 ± 0.5^{c}	18.3 ± 0.6	-11.9 ± 0.1^{b}	55.4 ± 4.8	-22.5 ± 0.4^{a}	26.2 ± 4.2	0
PLA/PCM	0	-9.7 ± 0.1^{bc}	-23.4 ± 0.3^{d}	88.9 ± 5.9	-38.0 ± 4.2^{c}	11.1 ± 5.9	-	-	13.6 ± 0.3
	5	-10.3 ± 0.8^{c}	-22.1 ± 1.9^{d}	70.4 ± 1.6	-32.5 ± 2.3^{c}	28.4 ± 1.6	-37.0 ± 0.51^{b}	1.2 ± 0.3	11.8 ± 2.5
	10	-9.4 ± 0.3^{abc}	-12.7 ± 0.2^{a}	35.0 ± 2.1	-23.4 ± 0.1^{a}	37.2 ± 3.2	-31.2 ± 0.8^{c}	27.8 ± 5.3	3.3 ± 0.2

T_m: Melting temperature; ΔH: % of latent heat released at each crystallization temperature. T_{c1}, T_{c2}, T_{c3}: crystallization temperatures.
[a-d]Different superscripts within a column indicate significant differences among samples ($P < 0.05$).

ACKNOWLEDGMENTS

A. Lopez-Rubio and M. J. Fabra are recipients of a Ramon y Cajal contract and a Juan de la Cierva contract, respectively from the Spanish Ministry of Economy and Competitivity. The authors would like to acknowledge the EU project of the FP7 FRISBEE for financial support.

REFERENCES

1. Sharma, A.; Tyagi V. V.; Chen, C. R.; Buddhi, D. *Renew. Sustain. Energy Rev.* **2009**, *13*, 318.
2. Alkan, C.; Sari, A.; Karaipekli, A. *Energy Convers. Manag.* **2011**, *52*, 687.
3. Li, D.; Xia, Y. *Adv. Mater.* **2004**, *16*, 1151.
4. Yamagishi, Y.; Sugeno, T.; Ishige, T.; Takeuchi, H.; Pyatenko, A.T. *Energy Conversion Engineering Conference. Proceedings of the 31st Intersociety* **1996**, *3*, 2077.
5. Miyoshi, T.; Toyohara, K.; Minematsu, H. *Polym. Int.* **2005**, *54*, 1187.
6. Chen, Y.; Xinsong, L.; Tangying, S. *J. Appl. Polym. Sci.* **2007**, *103*, 380.
7. Jiang, H.; Zhao, P.; Zhu, K. *Macromol. Biosci.* **2007**, *7*, 517.
8. Torres-Giner, S.; Gimenez, E.; Lagaron, J. M. *Food Hydrocolloids* **2008**, *22*, 601.
9. Fernandez, A.; Torres-Giner, S.; Lagaron, J. M. *Food Hydrocolloids* **2009**, *23*, 1427.
10. Torres-Giner, S.; Martínez-Abad, A.; Ocio, M. J.; Lagaron, J. M. *J. Food Sci.* **2010**, *75*, N69.
11. Perez-Masia, R.; Lopez-Rubio, A.; Lagaron, J. M. *Food Hydrocolloids* **2013**, *30*, 182.

12. Pamula, E.; Menaszek, E. *J. Mater. Sci.: Mater. Med.* **2008**, *19*, 2063.
13. Cohn, D.; Hotovely Salomon, A. *Biomaterials* **2005**, *26*, 2297.
14. Huang, M. H.; Li, S.; Vert, M. *Polymer* **2004**, *45*, 8675.
15. Garkhal, K.; Verma, S. *J. Polym. Sci. Part A: Polym. Chem.* **2007**, *45*, 2755.
16. Haroosh, H. J.; Chaudhary, D. S.; Dong, Y. *J. Appl. Polym. Sci.* **2012**, *124*, 3930.
17. Wang, B. Y.; Fu, S. Z.; Ni, P. Y.; Peng, J. R.; Zheng, L.; Luo, F.; Liu, H.; Qian, Z. Y. *J. Biomed. Mater. Res. Part A* **2012**, *100 A*, 441.
18. Buschle-Diller, G.; Cooper, J.; Xie, Z.; Wu, Y.; Waldrup, J.; Ren, X. *Cellulose* **2007**, *14*, 553.
19. Zahedi, P.; Karami, Z.; Rezaeian, I.; Jafari, S. H.; Mahdaviani, P; Abdolghaffari, A. H.; Abdollahi, M. *J. Appl. Polym. Sci.* **2012**, *124*, 4174.
20. P201131063 Patent Application. *Procedimiento de encapsulación de PCMs.* Inventors: Lagaron, J. M., Perez-Masia, R., & Lopez-Rubio, A. Holder entity: CSIC, **2011**.
21. Kishimoto, A.; Setoguchi, T.; Yoshikawa, M.; Nakahira, T. *Proceedings of 16th Japan Symposium on Thermophysical Properties,* **1995**.
22. Senador, A. E.; Shaw, M. T.; Mather, P. T. *Mater. Res. Soc. Symp. Proc.* **2001**, *661*, KK591.
23. Desai, K.; Kit, K.; Li, J.; Zivanovic, S. *Biomacromolecules* **2008**, *9*, 1000.
24. Shi, H., Zhao, Y., Zhang, X., Jiang, S., Wang, D., Han, C. C., Xu, D. *Macromolecules* **2004**, *37*, 9933.
25. Gnatyuk, I. I.; Platonova, N. V.; Puchkovskaya, G. A.; Kotelnikova, E. N.; filatov, S. K.; Baran, J. Drozd, M. *J. Struct. Chem.* **2007**, *48*, 654.
26. Sasaki, K., Inayoshi, N., Tashiro, K. *J. Phys. Chem. C* **2009**, *113*, 3287.
27. Makarenko, S. P., Puchkovska, G. A., Kotelnikova, E. N., Filatov, S. K. *J. Mol. Struct.* **2004**, *704*, 25.
28. Nichols, M. E.; Robertson, R. E. *J. Polym. Sci. Part B: Polym. Phys.* **1992**, *30*, 305.
29. Mathot, V. B. F. In *Calorimetry and Thermal Analysis of Polymers.* Carl Hanser Verlag: Munnich, **1994**; p 232–297.
30. Zhang, X. X.; Fan, Y. F.; Tao, X. M. ; Yick, K. L. *Colloid Polym. Sci.* **2004**, *282*, 330.
31. Kraack, H.; Sirota, E. B.; Deutsch, M. *J. Chem. Phys.* **2000**, *112*, 6873.
32. Chan, A. K. C.; Hemmingsen, P. V.; Radosz, M. *J. Chem. Eng. Data* **2000**, *45*, 362.
33. Vieira, L. C.; Buchuid, M. B.; Lucas, E. F. *Energy Fuels* **2010**, *24*, 2208.
34. Touhtouh, S.; Becquart, F.; Taha, M. *J. Appl. Polym. Sci.* **2012**, *123*, 3145.
35. Espartero, J. L.; Rashkov, I.; Li, S. M.; Manlova, N.; Vert, M. *Macromolecules* **1996**, *29*, 3535.
36. Silverstein, R. M.; Webster, F. X.; Kiemle, D. In *Spectrometric Identification of Organic Compounds, 7th ed.* Wiley: USA, **2006**.
37. Phadungphatthanakoon, S.; Poompradub, S.; Wanichwecharungruang, S. P. *Appl. Mater. Interfaces* **2011**, *3*, 3691.
38. Fan, Y. F.; Zhang, X. X.; Wang, X. C.; Li, J.; Zhu, Q. B. *Thermochim. Acta* **2004**, *413*, 1.
39. Domanska, U.; Rolinska, J. *Fluid Phase Equilibria* **1993**, *86*, 233.
40. http://energain.co.uk.
41. http://www.basf.com/group/corporate/en/brand/MICRONA_PCM.